Article

Cell Reports

Conditional Loss of *Pten* in Myogenic Progenitors Leads to Postnatal Skeletal Muscle Hypertrophy but Age-Dependent Exhaustion of Satellite Cells

Graphical Abstract

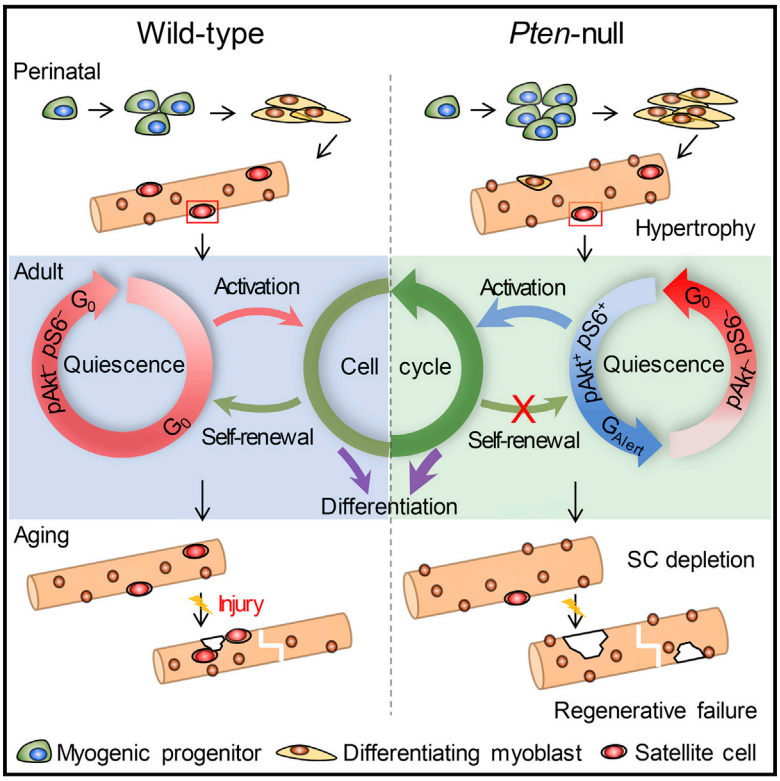

Authors

Feng Yue, Pengpeng Bi, Chao Wang, Jie Li, Xiaoqi Liu, Shihuan Kuang

Correspondence

skuang@purdue.edu

In Brief

Yue et al. find that Pten is required for muscle stem cell (satellite cell) homeostasis. *Pten* deletion in embryonic myogenic progenitors leads to a reduction of postnatal satellite cells that are in an "alert" state. These G_{Alert} satellite cells are defective in self-renewal and depleted with age, leading to regenerative failure.

Highlights

- Loss of *Pten* in myoblasts leads to postnatal muscle hypertrophy
- *Pten* null satellite cells are maintained in an "alert" state in adult resting muscle
- *Pten* null satellite cells are defective in self-renewal and cannot reenter quiescence
- *Pten* null G_{Alert} satellite cells are depleted with age, leading to regenerative failure

Yue et al., 2016, Cell Reports *17*, 2340–2353
November 22, 2016
http://dx.doi.org/10.1016/j.celrep.2016.11.002

OPEN ACCESS
CellPress

Cell Reports
Article

Conditional Loss of *Pten* in Myogenic Progenitors Leads to Postnatal Skeletal Muscle Hypertrophy but Age-Dependent Exhaustion of Satellite Cells

Feng Yue,[1] Pengpeng Bi,[1] Chao Wang,[1] Jie Li,[2] Xiaoqi Liu,[2,3] and Shihuan Kuang[1,3,4,*]
[1]Department of Animal Sciences
[2]Department of Biochemistry
[3]Center for Cancer Research
Purdue University, West Lafayette, IN 47907, USA
[4]Lead Contact
*Correspondence: skuang@purdue.edu
http://dx.doi.org/10.1016/j.celrep.2016.11.002

SUMMARY

Skeletal muscle stem cells (satellite cells [SCs]) are normally maintained in a quiescent (G_0) state. Muscle injury not only activates SCs locally, but also alerts SCs in distant uninjured muscles via circulating factors. The resulting G_{Alert} SCs are adapted to regenerative cues and regenerate injured muscles more efficiently, but whether they provide any long-term benefits to SCs is unknown. Here, we report that embryonic myogenic progenitors lacking the phosphatase and tensin homolog (*Pten*) exhibit enhanced proliferation and differentiation, resulting in muscle hypertrophy but fewer SCs in adult muscles. Interestingly, *Pten* null SCs are predominantly in the G_{Alert} state, even in the absence of an injury. The G_{Alert} SCs are deficient in self-renewal and subjected to accelerated depletion during regeneration and aging and fail to repair muscle injury in old mice. Our findings demonstrate a key requirement of Pten in G_0 entry of SCs and provide functional evidence that prolonged G_{Alert} leads to stem cell depletion and regenerative failure.

INTRODUCTION

Skeletal muscles are mainly composed of multinucleated muscle cells called myofibers. Generation of myofibers occurs during embryonic and fetal myogenesis through fusion of myogenic progenitors (myoblasts) that express Pax3/7 and MyoD (Gros et al., 2005; Relaix et al., 2005). Meanwhile, a subpopulation of myoblasts is deposited along the newly formed myofibers. These cells lose the expression of MyoD and Pax3 and become $Pax7^+$-quiescent satellite cells (SCs), the resident muscle stem cells (Tajbakhsh, 2009). By the perinatal stage, the number of myofibers is determined and remains constant, but the size of myofibers grows robustly with the addition of new myonuclei, which are supplied from satellite cells (White et al., 2010; Yin et al., 2013).

Adult resting skeletal muscle is relatively stable but possesses a remarkable ability to regenerate after injury (Brack and Rando, 2012; Cheung and Rando, 2013; Yin et al., 2013). Muscle regeneration is a highly orchestrated process involving crosstalk among tissues, cells, and molecules, and satellite cells are absolutely required for skeletal muscle regeneration (Lepper et al., 2011; Murphy et al., 2011; Sambasivan et al., 2011). In adult resting muscle, satellite cells are retained in a quiescent state, which is characterized by the expression of Pax7 (Kuang and Rudnicki, 2008). Upon muscle injury, quiescent satellite cells are activated and re-express MyoD and subsequently enter the cell cycle and proliferate (Kuang and Rudnicki, 2008). The proliferating satellite cells differentiate and fuse into multinucleated myofibers to repair the damaged muscles or self-renew to replenish the stem cell pool (Brack and Rando, 2012; Kuang and Rudnicki, 2008). During aging, the regenerative capacity of skeletal muscle declines due to functional declination of the systemic environment and satellite cells (Blau et al., 2015). Many intrinsic and extrinsic signals have been shown to govern the function of satellite cells, including Notch, Wnt, p38/MAPK, JNK/STAT, fibroblast growth factor (FGF), and many others (Almada and Wagers, 2016; Blau et al., 2015; Brack and Muñoz-Cánoves, 2016; Dumont et al., 2015).

Reversible transition of satellite cells between the quiescent and activated state is crucial for stem cell maintenance (Cheung and Rando, 2013). Deregulation of this process could result in abnormal growth of myogenic progenitors or depletion of satellite cells (Almada and Wagers, 2016; Cheung and Rando, 2013). Intriguingly, a recent study reports that quiescent satellite cells can be divided into reversible G_0 and G_{Alert} phases (Rodgers et al., 2014). In response to circulatory cues generated by injury, G_0 satellite cells, even in a remote uninjured muscle, transit into an alerted "G_{Alert}" state. Compared to G_0 satellite cells, the G_{Alert} satellite cells have higher mitochondrial activity and, when activated, enter the cell cycle more quickly and regenerate injured muscles more efficiently (Rodgers et al., 2014). Mechanistically, the cycling and metabolic features of the G_{Alert} state are dependent on mammalian target of rapamycin complex 1 (mTORC1) downstream of the phosphatidylinositol 3-kinase (PI3K) signaling pathway (Rodgers et al., 2014). Thus, the G_0 to G_{Alert} switch primes satellite cells to enter an adaptive stage,

allowing them to respond better to future injuries. However, it is unknown what signal regulates the opposite G_{Alert} to G_0 switch and if the G_{Alert} state provides any long-term benefits to stem cell maintenance and tissue homeostasis.

In the present study, we used *MyoD*^{Cre} to specifically delete the phosphatase and tensin homolog (*Pten*) in activated myoblasts and their descendants. Because Pten is a negative regulator of PI3K, we hypothesized that *Pten* deletion should lead to activation of downstream Akt-mTORC1 signaling and influence the differentiation and bidirectional switch between the activation and quiescence of myoblasts. We found that *MyoD*^{Cre}-driven deletion of *Pten* resulted in a spectrum of phenotypes in muscle tissue mass and satellite cell behavior, thus establishing the key role of Pten in regulating muscle stem cell homeostasis.

RESULTS

MyoD^{Cre}-Driven Deletion of *Pten* in Mice Results in Postnatal Muscle Hypertrophy

We established the *MyoD*^{Cre}::*Pten*$^{f/f}$ (*Pten*^{MKO}) mouse model to delete *Pten* specifically in MyoD-expressing embryonic myoblasts and their descendent satellite cells and myofibers. The *Pten*^{MKO} mice were born at normal Mendalian ratios, with normal morphology and body weight. However, the *Pten*^{MKO} mice outgrew their littermate wild-type (WT) mice during postnatal growth, resulting in heavier body weights and a larger body size starting at 10 weeks (Figures S1A–S1C). By contrast, heterozygous *MyoD*^{Cre}::*Pten*$^{+/f}$ (*Pten*$^{M+/-}$) mice were indistinguishable from WT mice (Figures S1B and S1C).

To determine if the increased body weight is due to increases in muscle mass, we examined various skeletal muscles. The tibialis anterior (TA), extensor digitorum longus (EDL), soleus (Sol), and gastrocnemius (Gas) muscles of adult *Pten*^{MKO} mice were larger and heavier than those of age-matched WT and *Pten*$^{M+/-}$ mice (Figures 1A–1C, S1D, and S1E). The increases in muscle size and weight in *Pten*^{MKO} mice were also apparent in juvenile mice at P7 (Figures S1F and S1G), before manifestation of a significant increase in body weight (Figure S1A). Histologically, *Pten*^{MKO} myofibers appeared larger in TA, EDL, and Sol cross-sections (Figures 1D and S1H), and the cross-sectional area (CSA) distribution curve of *Pten*^{MKO} Sol myofibers showed a right shift when overlaid to that of WT mice (Figure 1E), indicating a larger myofiber size. In addition, *Pten*^{MKO} mice had 15% and 10% more myofibers than did WT control mice in TA and EDL muscles, respectively (Figure 1F). Moreover, *Pten*^{MKO} EDL myofibers contained ~30% more myonuclei/myofiber than did the WT and *Pten*$^{M+/-}$ myofibers (Figures 1G and S1I). Taken together, these results indicate that *Pten* loss in embryonic myoblasts leads to increases in skeletal muscle mass due to myofiber hypertrophy (increases in size and myonuclei number per myofiber) and hyperplasia (increases in myofiber numbers).

Pten^{MKO} Mice Have Improved Skeletal Muscle Function and Are Protected from Denervation-Induced Muscle Atrophy

To explore if muscle hypertrophy is associated with functional improvements in *Pten*^{MKO} mice, we first examined their exercise performance on a treadmill. Both male and female *Pten*^{MKO} mice outperformed the sex-matched WT littermates in maximum speed, running time, and running distance (Figures 2A–2C). We also investigated the retention of muscle mass after denervation, and found that denervation-induced muscle loss was reduced in *Pten*^{MKO} mice compared to WT controls (Figure 2D). At 21 days after denervation, the weights of TA and Gas muscles were reduced by ~50% in control mice but by ~40% in *Pten*^{MKO} mice (Figure 2E). The denervated myofibers were also larger in *Pten*^{MKO} mice than in WT mice (Figures 2F and 2G). Importantly, the preservation index (size ratio of denervated to control muscles) in *Pten*^{MKO} mice was significant higher than that of WT mice (Figure 2H). Thus, loss of *Pten* improves skeletal muscle function and alleviates denervation-induced atrophy.

Loss of *Pten* Accelerates Proliferation and Differentiation of Satellite Cells during Perinatal Muscle Growth

During perinatal development, myofibers grow via nuclei accretion from satellite cells (White et al., 2010; Yin et al., 2013). The finding of increased myonuclei in *Pten*^{MKO} mice prompted us to hypothesize that *Pten* deletion promotes the proliferation and differentiation of satellite cells during perinatal muscle growth. To test this, we first examined the abundance of satellite cells in hindlimb muscles of newborn mice (P1) by immunostaining of Pax7. Indeed, we detected more Pax7$^+$ cells per unit area in TA muscles of *Pten*^{MKO} mice (Figure 3A), with a 51% increase over WT controls (Figure 3B). The number of Pax7$^+$Ki67$^+$ cells in *Pten*^{MKO} muscles was doubled compared to that of WT controls (Figures 3A and 3C), indicating that *Pten* deletion accelerates the proliferation of satellite cells. Moreover, more MyoG$^+$ cells were observed in muscles of newborn *Pten*^{MKO} mice (Figure 3D), corresponding to a 68% increase over WT controls (Figure 3E). The protein levels of Pax7, MyoG, pAkt, and CCND1 were consistently higher in the skeletal muscles of P7 *Pten*^{MKO} mice than in those of WT mice (Figure 3F). These results reveal that *Pten* deletion induces the postnatal skeletal muscle hypertrophy by promoting proliferation and differentiation of satellite cells during perinatal growth.

Pten Negatively Regulates Proliferation and Differentiation of Primary Myoblasts In Vitro

To confirm the observations in vivo, we investigated the function of Pten in satellite-cell-derived primary myoblasts through loss-of-function and gain-of-function approaches. The *Pten*-deficient primary myoblasts grew significant faster than the control myoblasts (Figure S2A). Single cell colony formation assay showed that the colony size of *Pten* null primary myoblasts was larger than control colonies (Figure S2B). The mRNA levels of the mitotic-related genes *Cdk2*, *Ccnd1*, and *Ccnd2* were significantly higher in *Pten* null myoblasts compared to WT myoblasts (Figure S2C). The protein levels of pAkt, pS6, and CCND1 were also increased in primary myoblasts after *Pten* deletion (Figure S2D). However, the protein levels of Pax7, MyoD, and MyoG were comparable in control and *Pten* KO myoblasts (Figure S2D).

In contrast to *Pten*-deficient myoblasts, *Pten*-overexpressing myoblasts exhibited significantly slower growth kinetics that did the control myoblasts infected with Ad-GFP (Figure S2E). Immunostaining confirmed that *Pten*-overexpressing myoblasts were mostly Ki67$^-$, which resulted in a much lower percentage

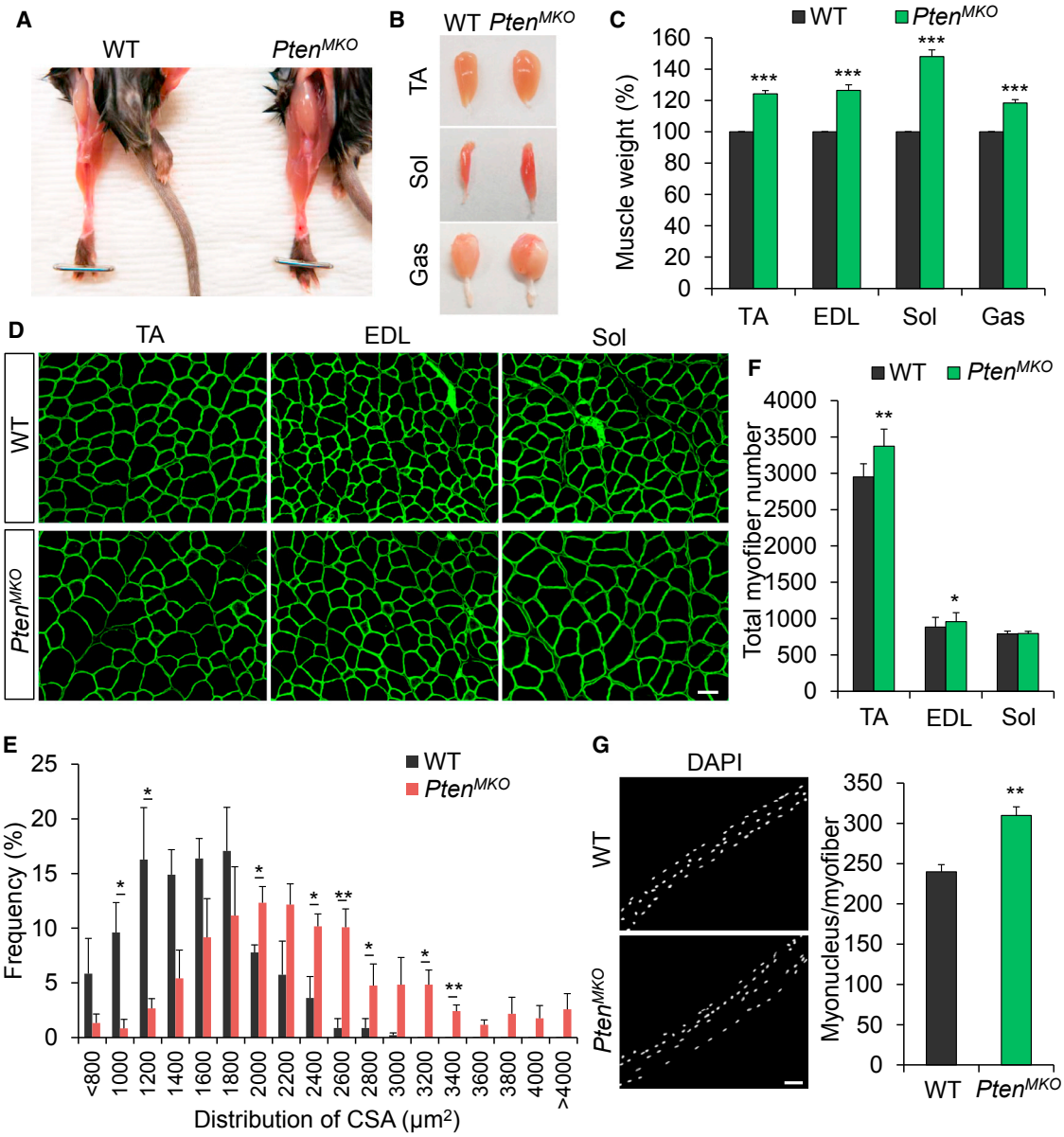

Figure 1. *Pten* Deletion in Myogenic Progenitors Leads to Postnatal Muscle Hypertrophy

(A and B) Representative image of whole hind limb (A) and TA, Sol, and Gas muscles (B) in adult WT and *Pten*^{MKO} mice.

(C) Muscle weight in adult WT and *Pten*^{MKO} mice (n = 7).

(D) Dystrophin staining showing relative size of myofibers in muscle cross-sections.

(E) Frequency of distribution for CSA (μm^2) of Sol muscle (n = 4).

(F) Total myofiber number of TA, EDL, and Sol muscles (n = 4–8).

(G) Immunofluorescence of DAPI and myonucleus number count in fresh myofibers (n = 4 mice, 20 myofibers per mouse).

Scale bar, 50 μm. Data are shown as mean ± SEM (t test: *p < 0.05; **p < 0.01; ***p < 0.001). See also Figure S1.

of Ki67$^-$ myoblasts compared to control myoblasts (Figure S2F). Moreover, the mRNA levels of *MyoD*, *MyoG*, and *Ccnd1* were significantly downregulated by Pten overexpression (Figure S2G), so was the protein level of MyoG (Figure S2H). Importantly, *Pten*-overexpressing myoblasts failed to differentiate into myotubes, whereas the Ad-GFP-infected control myoblasts differentiated efficiently (Figure S2I). Together, these results demonstrate that Pten negatively regulates the proliferation and differentiation of primary myoblasts.

Satellite Cells in Adult *Pten*^{MKO} Mice Are Predominantly at the G_{Alert} State

Because satellite cells are derived from embryonic MyoD-expressing myoblasts (Kanisicak et al., 2009), we next examined

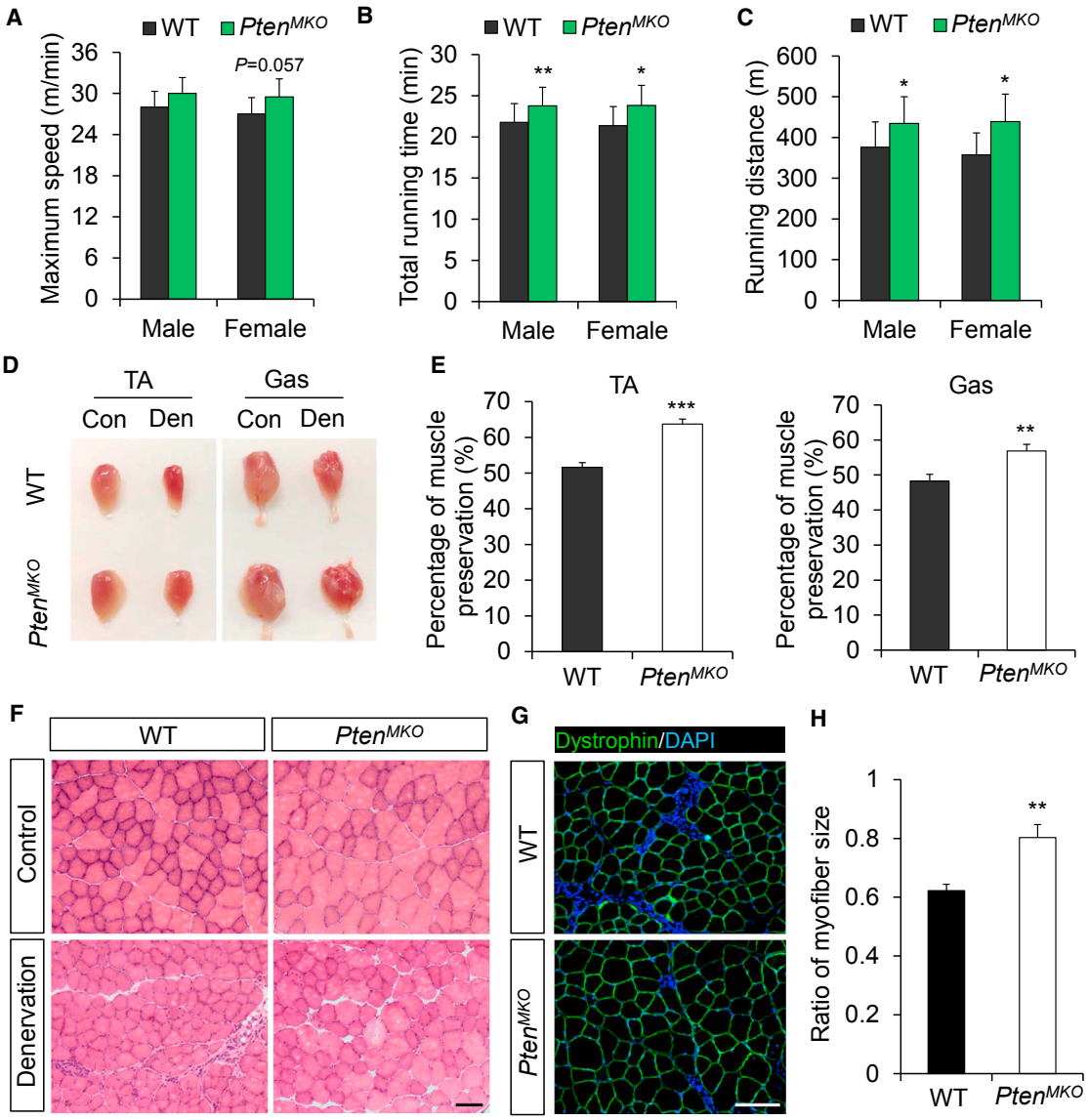

Figure 2. Loss of *Pten* Improves Skeletal Muscle Function and Protects Muscle from Denervation-Induced Atrophy

(A–C) Maximum speed (A), total running time (B), and running distance (C) of adult WT and *Pten*^{MKO} female and male mice measured by treadmill (n = 3).

(D and E) Representative image (D) and percentage of muscle preservation (E) of TA and Gas muscles 21 days post denervation (n = 6).

(F and G) H&E (F) and immunofluorescence (G) staining of TA muscles 21 days post denervation.

(H) Ratio of myofiber size (ratio of denervation to control) 21 days post denervation (n = 5).

Scale bar, 50 μm. Data are shown as mean ± SEM (t test: *p < 0.05; **p < 0.01; ***p < 0.001).

how *Pten* KO affects satellite cells in adult *Pten*^{MKO} mice. To determine *Pten* KO efficiency, we double labeled satellite cells with Pax7 and Pten (Figure 4A). All (100%) Pax7^{+} satellite cells were Pten^{+} in WT muscles, but only less than 6% of Pax7^{+} satellite cells were Pten^{+} in *Pten*^{MKO} muscles (Figure 4A), suggesting *Pten* deletion in >94% of adult satellite cells. Strikingly, the number of Pax7^{+} satellite cells in adult *Pten*^{MKO} mice was only ~60% of that in WT mice (Figure 4B). Fluorescence-activated cell sorting (FACS) analysis of satellite cells isolated from quadriceps muscles confirmed that both the number (5188/muscle versus 6822/muscle) and percentage (4.3% versus 7.9%) of Pax7^{+} satellite cells were decreased in adult *Pten*^{MKO} mice compared to WT mice (Figures S3A and S3B).

The reduction in satellite cell numbers in *Pten*^{MKO} mice suggests that *Pten* null embryonic myoblasts are defective in forming quiescent satellite cells or *Pten* null satellite cells cannot maintain proper quiescence. To distinguish these possibilities, we investigated the cell cycle status of satellite cells in adult *Pten*^{MKO} mice. By immunostaining of MyoD (marker of activated satellite cells) and MyoG (marker of differentiating myoblasts) in freshly isolated myofibers, we found that there were essentially no MyoD^{+} or MyoG^{+} cells in both WT and

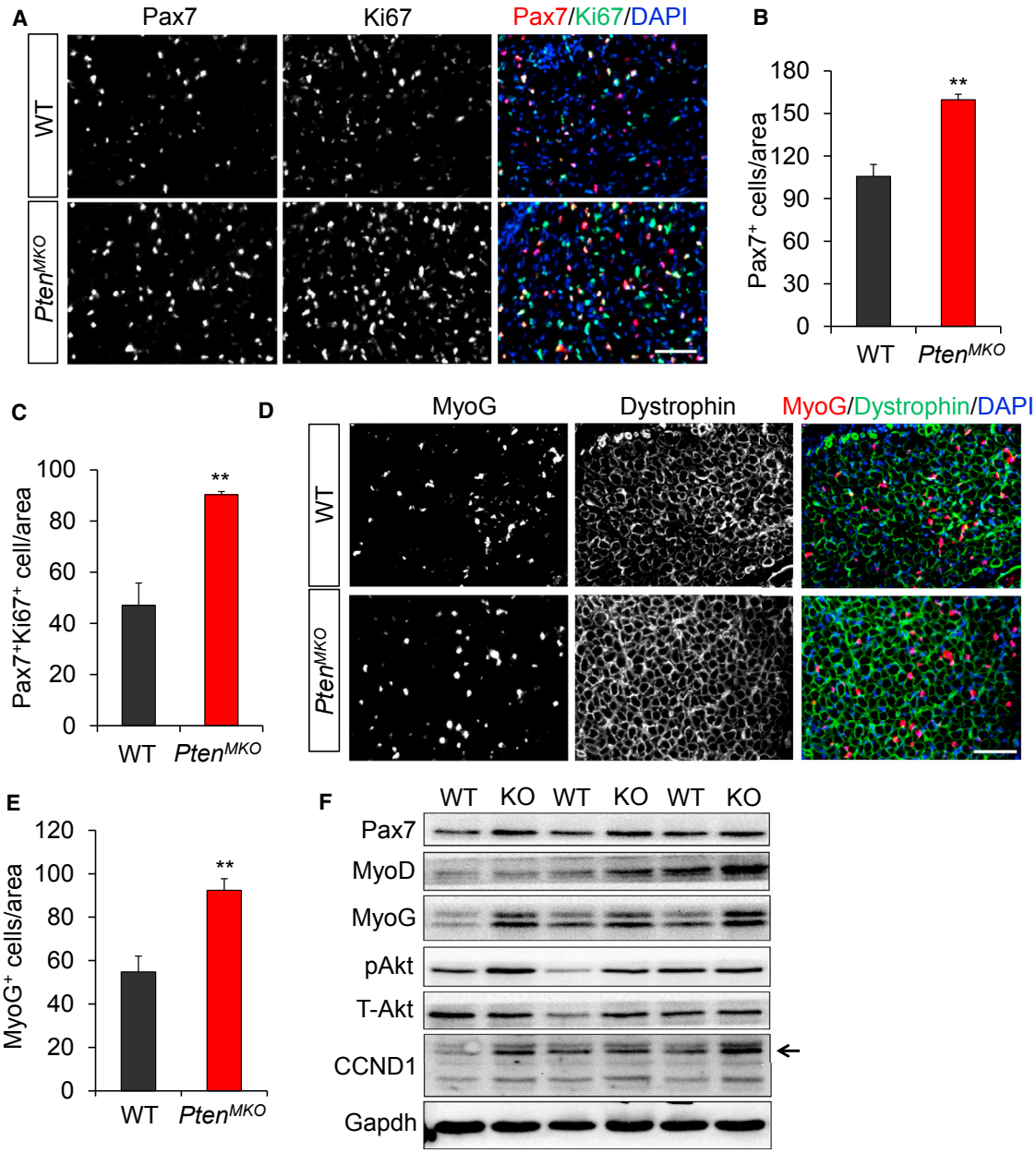

Figure 3. *Pten* Deletion Promotes Satellite Cell Proliferation and Differentiation during Perinatal Muscle Growth

(A) Immunofluorescence of Pax7 and Ki67 in cross-sections of hind limb muscles from newborn (P1) WT and *Pten*^{MKO} mice.

(B and C) Quantification of Pax7^{+} cell (B) and Pax7^{+}Ki67^{+} cell (proliferating) (C) number in cross-sections of hind limb muscles (n = 3).

(D) Immunofluorescence of MyoG and dystrophin in cross-sections of hind limb muscles.

(E) Quantification of MyoG^{+} cell number in cross-sections of hind limb muscles (n = 3).

(F) Western blot analysis of myogenic and proliferating markers in skeletal muscles from P7 mice. Arrow indicates the right band.

Scale bar, 50 μm. Data are shown as mean ± SEM (t test: *p < 0.05; **p < 0.01). See also Figure S2.

Pten^{MKO} mice at 2.5 and 8 months (Figures S3C and S3D). Immunostaining of the proliferating marker Ki67 consistently confirmed that no satellite cells in *Pten*^{MKO} and WT mice were Ki67^{+} (Figure S3E). These results suggest that the *Pten*-deficient satellite cells in the *Pten*^{MKO} mice are maintained in a quiescent state.

It has recently been shown that quiescent satellite cells exist at two functional distinct phases: G_0 and G_{Alert} (Rodgers et al., 2014). One feature of G_{Alert} satellite cells is their accelerated activation and proliferation kinetics. On the basis of 5-ethynyl-2′-deoxyuridine (EdU) incorporation in myofibers cultured ex vivo, we found that *Pten*^{MKO} satellite cells displayed accelerated cell

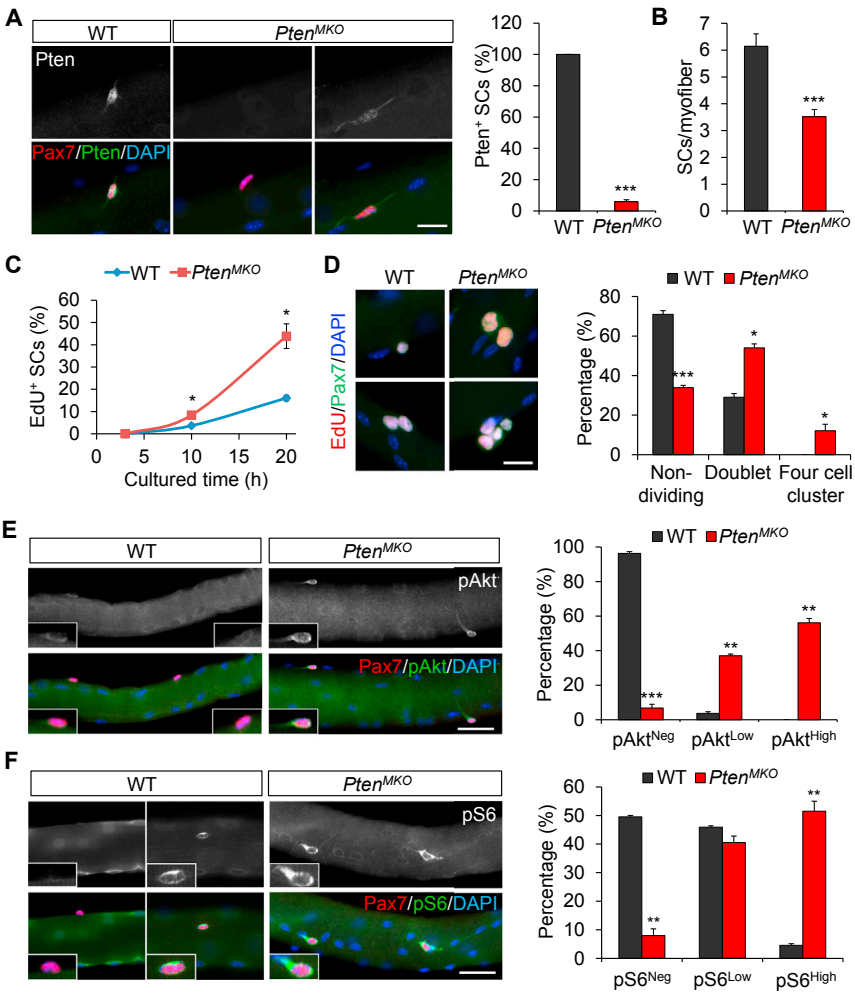

Figure 4. Quiescent Satellite Cells Exist in an "Alert"—G_{Alert}—State in Adult *Pten*^{MKO} Mice

(A) Immunofluorescence of Pax7 and Pten and percentage of Pten$^+$ satellite cells on fresh myofibers of adult WT and *Pten*^{MKO} mice (n = 4 mice, 20 myofibers per mouse).

(B) Quantification of satellite cell number on fresh myofibers (n = 7 mice, 20 myofibers per mouse).

(C) Cell cycle entry of satellite cells analyzed by EdU incorporation in cultured myofibers (n = 3 mice; an average of 100 satellite cells were counted per mouse).

(D) Immunofluorescence of Pax7 and EdU and percentage of proliferating satellite cells in myofibers cultured for 40 hr (n = 3 mice, 15 myofibers per mouse).

(E) Immunofluorescence of pAkt in Pax7$^+$ satellite cells and percentages of pAkt^{Neg}, pAkt^{Low}, and pAkt^{High} satellite cells on fresh myofibers (n = 3 mice, 20 myofibers per mouse).

(F) Immunofluorescence of pS6 in Pax7$^+$ satellite cells and percentages of pS6^{Neg}, pS6^{Low}, and pS6^{High} satellite cells on fresh myofibers (n = 3 mice, 20 myofibers per mouse).

Scale bar, 20 μm. Data are shown as mean ± SEM (t test: *p < 0.05; **p < 0.01; ***p < 0.001). See also Figure S3.

cycle entry compared to WT satellite cells (Figure 4C). Specifically, >40% of *Pten*-deficient satellite cells had incorporated EdU (EdU$^+$) within 20 hr compared to <20% of EdU$^+$ satellite cells in WT mice at the same time (Figure 4C). At the clonal level, most *Pten*-deficient satellite cells had already divided one to two times in 40 hr, forming two to four cell clusters, whereas the WT satellite cells had only divided zero times to one time at the same time (Figure 4D). Another feature of G_{Alert} satellite cells is their metabolic activation. Using MitoTracker staining as a readout of mitochondria activity, we found that *Pten*-deficient quiescent satellite cells and primary myoblasts exhibited much more intensive MitoTracker labeling than did WT cells (Figures S3F and S3G). These results suggest that *Pten* null satellite cells are at the G_{Alert} state.

Activation of mTORC1 signaling has been shown to be necessary and sufficient to mediate the G_0 to G_{Alert} switch (Rodgers et al., 2014). To further confirm the G_{Alert} state of *Pten*-deficient satellite cells, we performed co-immunostaining of Pax7 with pAkt and pS6 downstream of mTORC1. Most quiescent satellite cells in WT muscles were negative for pAkt labeling (pAkt^{Neg}), whereas the *Pten* null satellite cells were predominantly pAkt$^+$, with low to high labeling intensity (Figure 4E). More intensive pS6 signals were also observed in the *Pten* null cells compared to the WT satellite cells (Figure 4F). Quantitatively, the percentages of pAkt^{Neg} and pS6^{Neg} satellite cells were remarkably decreased, but the percentages of pAkt^{Hi} and pS6^{Hi} satellite cells were dramatically increased in *Pten*^{MKO} mice (Figures 4E and 4F), suggesting activation of the mTORC1 pathway in *Pten*-deficient satellite cells. Together, these results indicate that *Pten* deletion in embryonic myoblasts renders the satellite cell at the G_{Alert} state.

G_{Alert} Satellite Cells Efficiently Regenerate Injured Muscles in Young Mice at the Expense of Self-Renewal

We next asked if the reduced number of G_{Alert} satellite cells in *Pten*^{MKO} mice could maintain muscle regeneration after cardiotoxin (CTX)-induced muscle injury (Figure 5A). Strikingly, no significant differences were found between WT and *Pten*^{MKO} mice in gross morphology and muscle weight recovery 7 days after injury (Figures 5B and 5C). In addition, cross-sections of both WT and *Pten*^{MKO} muscles displayed similar levels of inflammatory infiltration, regeneration (central nuclear myofibers), and dystrophin expression (Figures 5D and 5E). At 21 days after injury, regenerated myofibers in *Pten*^{MKO} mice remained larger than those of WT mice (Figures 5D and 5E). These results suggest that the reduce numbers of G_{Alert} satellite cells in adult *Pten*^{MKO} mice are sufficient to maintain muscle regeneration after acute injury.

We also examined the dynamics of the G_{Alert} satellite cells during muscle regeneration. Prior to muscle injury (day 0), the

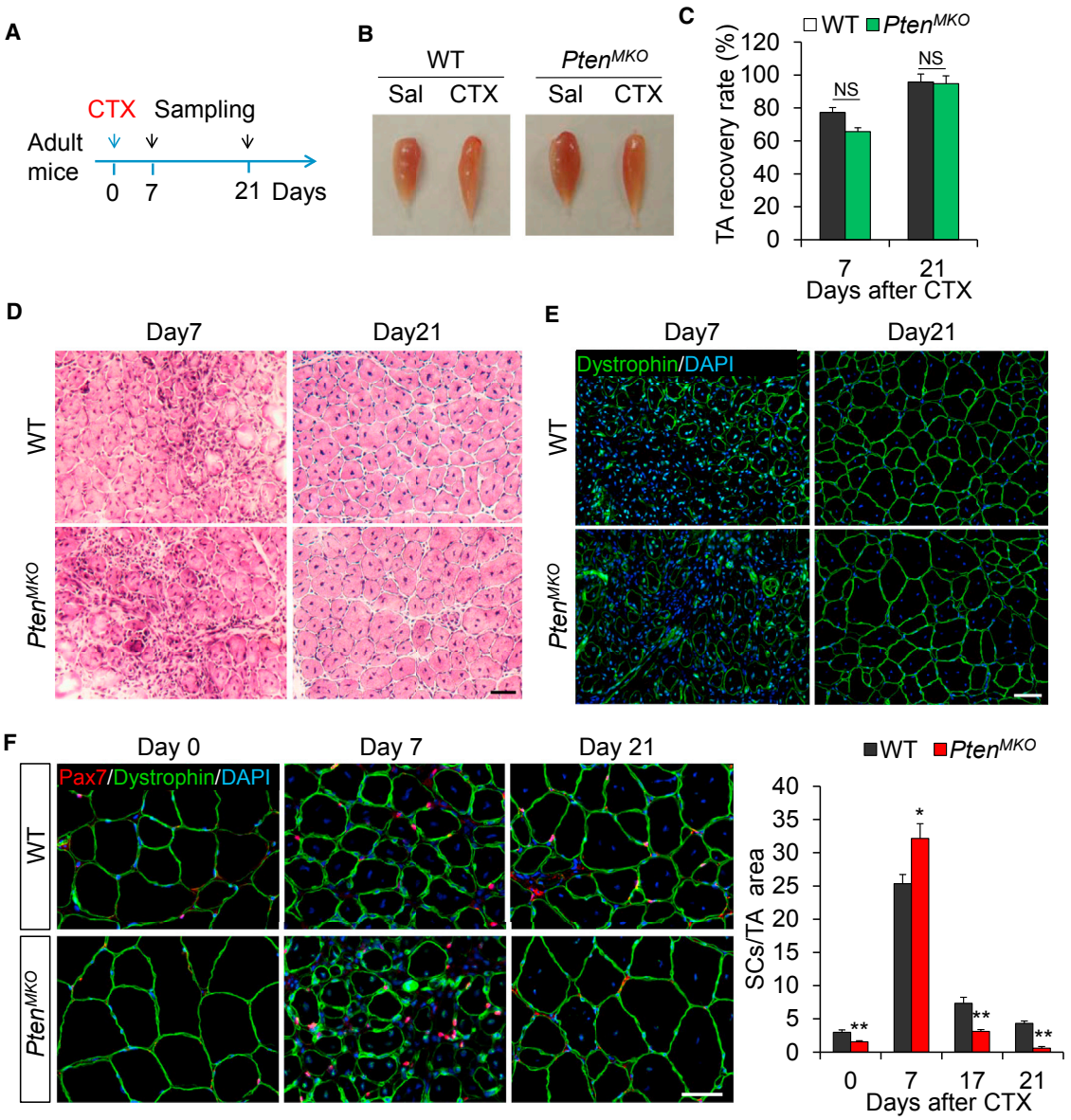

Figure 5. G_{Alert} Satellite Cells Are Able to Maintain Muscle Regeneration at the Expense of Self-Renewal in Young *Pten*^{MKO} Mice

(A) Schematic outline of CTX injection and sample collection.

(B and C) Representative images (B) and recovery rate (C) of TA muscles in young WT and *Pten*^{MKO} mice at 7 and 21 days after injury (n = 3).

(D) H&E staining of TA muscle cross-sections.

(E) Immunofluorescence of dystrophin in TA cross-sections.

(F) Immunofluorescence of Pax7 and dystrophin and satellite cell number per area of TA cross-sections (n = 3–6).

Scale bar, 50 μm. Data are shown as mean ± SEM (t test: *p < 0.05; **p < 0.01; ***p < 0.001; NS, no significant difference). See also Figures S4 and S5.

number of Pax7^{+} satellite cells in *Pten*^{MKO} mice was only ~50% of that in WT mice, but there were significantly more satellite cells in *Pten*^{MKO} muscles than in WT muscles at day 7 after injury (Figure 5F). This result suggests that *Pten*^{MKO} satellite cells respond more quickly to injury and proliferate faster than do the WT satellite cells. At day 17 and 21, when muscle regeneration gradually finishes, proliferating satellite cells exit the cell cycle and return to quiescence (Yin et al., 2013). Intriguingly, significantly fewer satellite cells were found in *Pten*^{MKO} muscles than in WT muscles at day 17 and 21 after injury, with only 14% of that in WT muscles at day 21 (Figure 5F). This observation indicates that initial faster proliferation of the G_{Alert} satellite cells is associated with reduced self-renewal and therefore exacerbates satellite cell loss in *Pten*^{MKO} mice after regeneration.

To exclude the effect of hypertrophic myofiber niche on the response of satellite cells to injury, we generated *Pax7*^{CreER}/*Pten*$^{f/f}$ mice to achieve acute deletion of *Pten* in adult satellite cells. At 12 days after tamoxifen-induced deletion of *Pten*, the

number of satellite cells in TA muscles was decreased by 58% (Figures S4A and S4B), suggesting that Pten is required for maintaining quiescent satellite cells in resting muscles. We also examined satellite cell self-renewal and muscle repair during injury (Figure S4C). Similar to what we found in $Pten^{MKO}$ mice, TA muscles of $Pax7^{CreER}/Pten^{f/f}$ mice regenerated normally, despite the nearly 60% loss of satellite cells prior to injury (Figures S4D and S4E). Notably, a more pronounced reduction of satellite cells in injured TA muscles of $Pax7^{CreER}/Pten^{f/f}$ mice was observed 7 days after CTX injection (Figure S4F), a pattern similar to the loss of satellite cells during muscle regeneration in $Pten^{MKO}$ mice. These results indicate that Pten is required for the self-renewal of activated satellite cells in a cell-autonomous manner that is independent of the hypertrophic myofiber niche.

Disruption of *Pten* Affects the Reversible Quiescence of Satellite Cell Progenitors

A failure of the *Pten null* satellite cells to replenish their pool after muscle regeneration might be due to programmed cell death. To test this possibility, we used terminal deoxynucleotidyl transferase dUTP nick-end labeling (TUNEL) assay to detect apoptotic cells. $TUNEL^+$ cells were observed in injured TA muscles in both WT and $Pten^{MKO}$ mice (Figure S5A). However, none of them were $Pax7^+$ in WT (n = 245 cells) and $Pten^{MKO}$ (n = 298 cells) mice (Figure S5A). No expression of active caspase3 was consistently found in $Pax7^+$ cells from WT (n = 95 cells) and $Pten^{MKO}$ (n = 82 cells) mice (Figure S5B). These results demonstrated that the depletion of satellite cells after regeneration was not due to cell apoptosis.

Alternatively, *Pten* might be required for activated satellite cells to return to quiescence, and the lack of *Pten* might have blocked their re-entry into the quiescent state. To examine this possibility, we analyzed the number of $Pax7^+MyoD^-$ quiescent satellite cells in TA muscles 10 days post muscle injury. As expected, the number of quiescent satellite cells was significantly reduced in $Pten^{MKO}$ mice than in WT controls, with a concomitant increase in the number of $Pax7^+MyoD^+$ activated myoblasts (Figure 6A). To confirm the in vivo results, we next performed "reserve" cell analysis in culture using low-passage primary myoblasts from $Pax7^{CreER}/Pten^{f/f}$ mice (Shea et al., 2010). Compared to the control media treatment, 4-OH-tamoxifen-induced *Pten* KO significantly reduced the percentage of $Pax7^+MyoD^-Ki67^-$ reserved cells (Figure 6B) and increased the percentages of $MyoG^+$ cells and nuclei in $MF20^+$ myotubes (Figures 6C and 6D). In addition, the expression of the differentiation-related genes *MyoG*, *Myh8*, *Cadh15*, and *Fndc5* was upregulated after *Pten* deletion (Figure 6E). These observations demonstrate that lack of *Pten* blocks the re-entry of activated satellite cells into quiescence and promotes their terminal differentiation.

We further asked whether the failure of cycling *Pten* null satellite cell progenitors to re-enter quiescence is due to the activation of Akt/mTOR signaling. To test this, we treated *Pten* KO and control myoblasts with LY294002 (a potent PI3K inhibitor) or rapamycin (a specific inhibitor of mTOR) in the low serum "reserve" cell culture condition. LY294002 and rapamycin treatment inhibited the differentiation and fusion of both control and *Pten* KO myoblasts (Figure S6A). Notably, LY294002 treatment increased the percentages of reserve cells ($Pax7^+MyoD^-Ki67^-$) in both the control and *Pten* KO group and rescued the defect of quiescence re-entry of *Pten* KO myoblasts (Figure S6B). Rapamycin similarly normalized the percentage of reserve cells in *Pten* KO cells to a level comparable to that of controls, although it decreased the overall percentage of reserve cells in both control and *Pten* KO myoblasts (Figure S6B). These observations suggest that inhibition of the Akt/mTOR pathway rescues the deficiency of *Pten* null myoblasts to re-enter quiescence. Collectively, these results indicate that Pten is required for the reversible quiescence of satellite cells.

Accelerated Depletion of G_{Alert} Satellite Cells during Aging Leads to Regenerative Failure

During aging, the number and function of satellite cells declines (Chakkalakal et al., 2012; Collins et al., 2007; Shefer et al., 2006). The observation that accelerated depletion of G_{Alert} satellite cells during muscle regeneration in young mice prompted us to ask whether the G_{Alert} satellite cells in $Pten^{MKO}$ mice could maintain the stem cell pool and regenerative capacity with age. To determine this, we first enumerated the number of satellite cells in resting muscles of 19-month-old WT and $Pten^{MKO}$ mice. Consistent with previous reports, a decline in satellite cells was observed in aged muscles (~2.5 satellite cells/myofiber) compared to young muscles (~6.2 satellite cells/myofiber) in WT mice (Figure 7A). Strikingly, there were almost no satellite cells (<1 cell/myofiber) in the 19-month-old $Pten^{MKO}$ mice (Figure 7A). Notably, ~25% of the satellite cells observed in $Pten^{MKO}$ mice were Pten positive (Figures S7A and S7B), suggesting that they were escapers of *Pten* deletion. Moreover, when cultured ex vivo for 3 days, clusters of proliferating satellite cells were observed on myofibers of WT mice, but rarely on myofibers of $Pten^{MKO}$ mice (Figure 7B). A dramatically reduced number of satellite cells was consistently observed in TA muscle cross-sections (Figure 7C). These results are indicative of accelerated depletion of *Pten*-deficient satellite cells with aging.

We next evaluated the regenerative capacity of old $Pten^{MKO}$ mice after CTX injury (Figure 7D). Even though the non-injured $Pten^{MKO}$ TA muscles remained larger than the WT muscles, the regenerated $Pten^{MKO}$ muscles were smaller than the WT muscles (Figure 7E). Although TA muscles of WT mice regenerated effectively, with ~80% of the recovery rate after injury, the $Pten^{MKO}$ muscles only recovered ~56% of their mass (Figure 7F). H&E staining revealed that whereas the WT muscle regenerated efficiently with homogeneous centrally nucleated myofibers, the $Pten^{MKO}$ muscles contained fewer regenerated myofibers and numerous densely packed nuclei, which were indicative of inflammatory infiltration (Figure 7G). Quantitatively, the average sizes of the myofibers were significantly reduced in $Pten^{MKO}$ muscles (Figure 7H). Labeling of the myofiber boundary with dystrophin confirms the existence of pockets of dystrophin-negative nuclei in the $Pten^{MKO}$ muscles but not in the WT muscles (Figure S7C). These data indicate that accelerated depletion of *Pten*-deficient G_{Alert} satellite cells during aging leads to regenerative defects.

DISCUSSION

Satellite cell dysfunction leads to failures of muscle repair, but the molecular mechanisms regulating satellite cell homeostasis

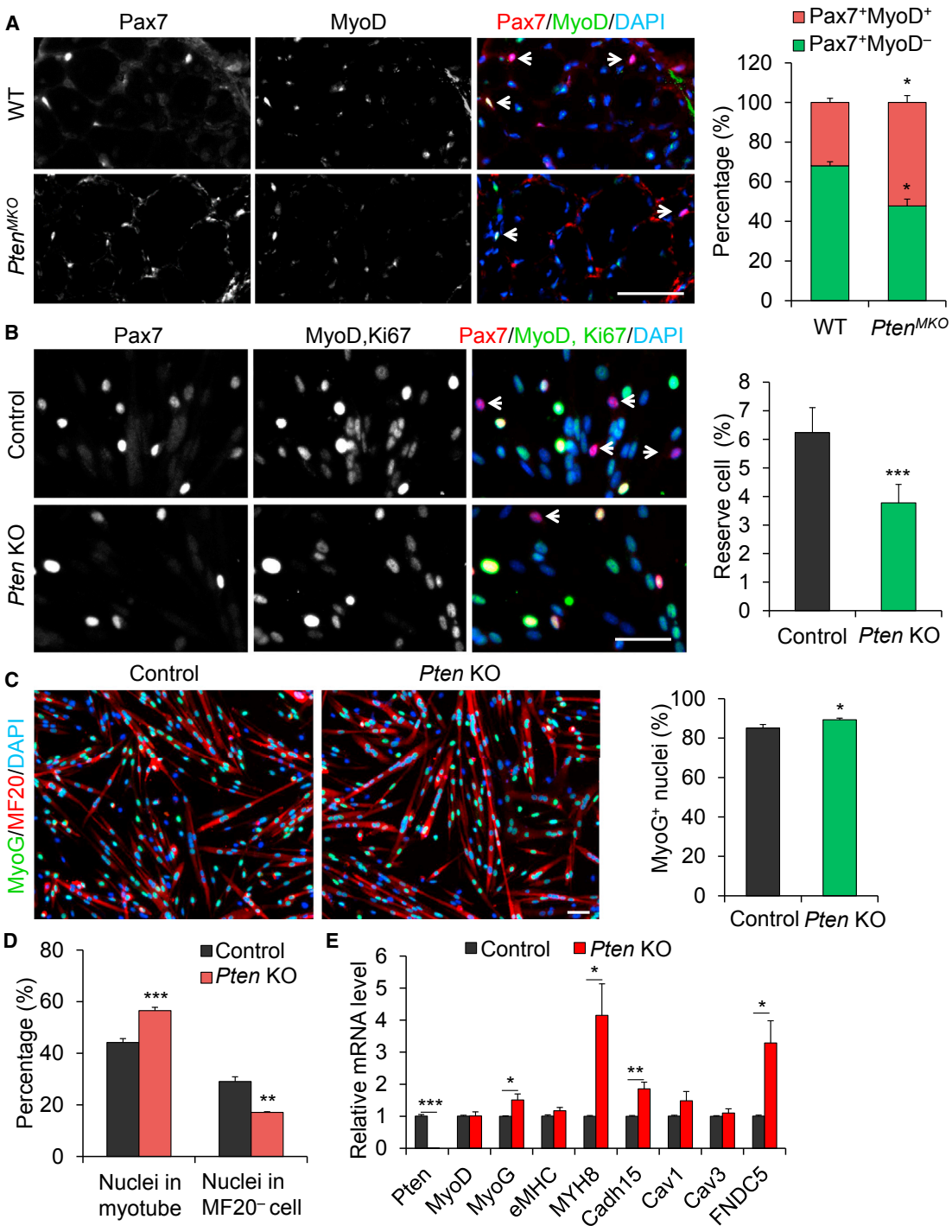

Figure 6. *Pten* KO Affects the Reversible Quiescence of Satellite Cell Progenitors

(A) Immunofluorescence of Pax7 and MyoD and percentage of $Pax7^{+}MyoD^{-}$ and $Pax7^{+}MyoD^{+}$ SCs in TA muscles of adult WT and $Pten^{MKO}$ mice after 10 days of CTX injury (n = 3 mice).

(B) Immunofluorescence of Pax7, MyoD, and Ki67 and percentage of $Pax7^{+}MyoD^{-}Ki67^{-}$ cells in cultures of control and *Pten* KO primary myoblasts after 2.5 days of differentiation to show reserved quiescent $Pax7^{+}$ cells (n = 6).

(C) Immunofluorescence of MyoG and MF20 and percentage of $MyoG^{+}$ nuclei in cultures (n = 4).

(D) Quantification of the percentage of nuclei in myotube and nuclei in $MF20^{-}$ cells in cultures (n = 4).

(E) RT-PCR analysis of gene expression in cultures (n = 3).

Scale bar, 50 μm. Data are shown as mean ± SEM (t test: *p < 0.05; **p < 0.01; ***p < 0.001). See also Figure S6.

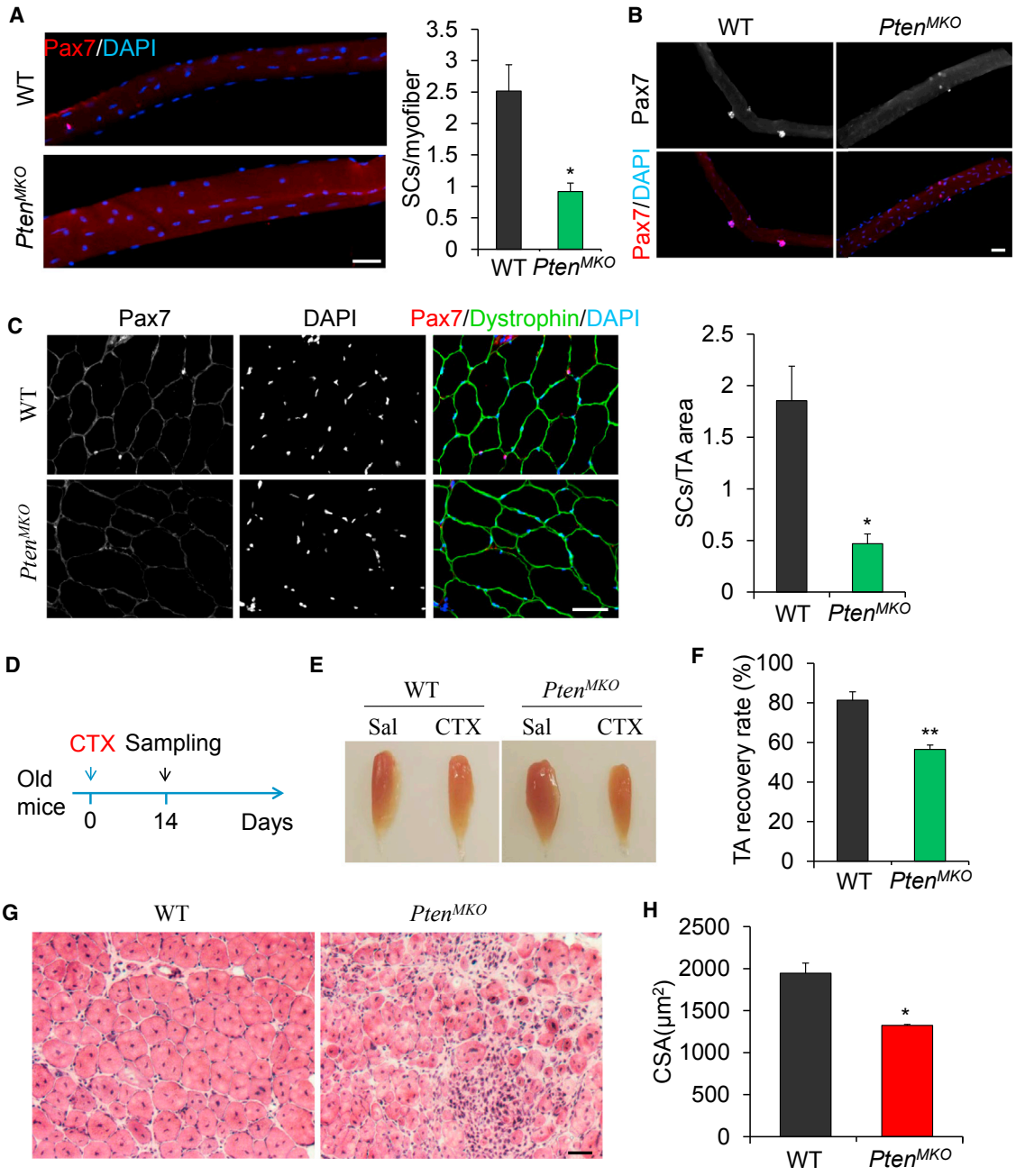

Figure 7. Depletion of G_{Alert} Satellite Cells in Aged Mice Impairs Muscle Regeneration

(A) Immunofluorescence of Pax7 and satellite cell number in fresh myofibers isolated from old WT and *Pten*^{MKO} mice (19 months, n = 3).

(B) Immunofluorescence of Pax7 in fresh isolated myofibers cultured for 3 days (n = 3).

(C) Immunofluorescence of Pax7 and dystrophin and satellite cell number per area of TA muscle cross-sections (n = 3).

(D) Schematic outline of CTX injection and sample collection.

(E and F) Representative images (E) and recovery rate (F) of TA muscles in old WT and *Pten*^{MKO} mice 14 days post injury (n = 3).

(G and H) H&E staining (G) and CSA per myofiber (H) of TA muscle cross-sections (n = 3).

Scale bar, 50 μm. Data are shown as mean ± SEM (t test: *p < 0.05; **p < 0.01). See also Figure S7.

remain poorly understood. Using the conditional knockout approach, our current study demonstrates that loss of *Pten* in embryonic myoblasts results in postnatal skeletal muscle hypertrophy, better motor function, and resistance to denervation-induced muscle atrophy. However, the *Pten*-KO-induced muscle hypertrophy is at the expense of disrupting the homeostasis of satellite cells by rendering them at the G_{Alert} state. This transiently promotes early postnatal muscle growth but accelerates

satellite cell exhaustion during aging. These findings point to a novel role of Pten in muscle progenitors and provide functional evidence that prolonged G_{Alert} leads to stem cell depletion and regenerative failure.

Activation of the PI3K/Akt pathway induces skeletal muscle hypertrophy by increasing protein synthesis (Bodine et al., 2001; Lai et al., 2004; Rommel et al., 2001). Thus, inactivation of Pten, which inhibits PI3K, should activate Akt and promotes muscle hypertrophy. However, myofiber-specific *Pten* KO driven by muscle creatine kinase (MCK)-Cre fails to induce muscle hypertrophy under normal conditions (Hamilton et al., 2010; Wijesekara et al., 2005). By contrast, we show that $MyoD^{Cre}$-driven *Pten* KO in myoblasts induces robust muscle hypertrophy. These observations suggest that muscle hypertrophy in our $Pten^{MKO}$ mice is mainly due to *Pten* deficiency in myoblasts but not in myofibers. Surprisingly, *Pten* KO driven by muscle and brown fat progenitor-specific $Myf5^{Cre}$ fails to elicit any muscle phenotypes (Sanchez-Gurmaches et al., 2012). Conversely, systemic overexpression of *Pten* increases energy expenditure due to improvements in brown adipose function, but the skeletal muscle phenotype of that mouse model is unclear (Ortega-Molina et al., 2012). Thus, the role of *Pten* in myogenic progenitors remained unknown. Our results demonstrate that *Pten* KO accelerates myoblast proliferation and differentiation during postnatal muscle growth and promotes myonuclei accretion and consequently muscle hypertrophy. Increased proliferation and fusion of satellite cells have been consistently shown to cause adult muscle hypertrophy by increasing the number of myonuclei (Serrano et al., 2008). Our results provide evidence that an adaptive increase of the number of myonuclei by *Pten* inactivation may preserve muscle mass under disease conditions, such as muscle atrophy.

A recent study reported that stem cell quiescence is composed of two distinct phases: G_0 and G_{Alert} (Rodgers et al., 2014). Stem cells undergo dynamic transitions from the G_0 to the G_{Alert} state in response to injury and stress. We show that *Pten* null satellite cells have elevated levels of pAkt and pS6 resembling the adaptive G_{Alert} stem cells. Supporting our results, activation of mTORC1 due to *TSC1* KO is sufficient to induce the G_0 to G_{Alert} switch in quiescent satellite cells (Rodgers et al., 2014). Because $MyoD^{Cre}$ induces *Pten* deletion in cycling (G1/M/G2 phase) embryonic myoblasts prior to the formation of quiescent (G_0) satellite cells, our results further indicate that Pten is necessary for G_0 entry of activated myoblasts during development. Our study and that of Rodgers et al. (2014) together demonstrate that the Akt/mTORC1 pathway is crucial for the bidirectional G_0/G_{Alert} switches. Whereas the previous study illustrates the mechanism for G_0 to G_{Alert} transition, our study now demonstrates that Pten is necessary for G_{Alert} to G_0 re-entry.

Despite the enhanced proliferative and regenerative capacity of G_{Alert} satellite cells, they are surprisingly depleted much more rapidly than G_0 satellite cells during regeneration and aging, resulting in regenerative failure in old mice. This observation indicates that G_{Alert} satellite cells have a shorter lifespan. Age-related depletion of the stem cell pool mainly results from deregulated stem cell homeostasis due to the loss of the self-renewal ability and activation of senescence pathways (Brack and Muñoz-Cánoves, 2016; Chakkalakal et al., 2012; Liu and Rando, 2011; Signer and Morrison, 2013; Sousa-Victor et al., 2015). Indeed, we find that G_{Alert} satellite cells have reduced the self-renewal ability. PI3K and its downstream mTORC1 pathways are essential regulators of stem cell aging and mammalian longevity (Johnson et al., 2013; Signer and Morrison, 2013). Hyperactivation of the mTORC1 pathway leads to enhanced mitochondrial activity, resulting in the increase of intracellular generation of reactive oxygen species, which cause DNA damage and cell senescence (Chen et al., 2008; Iglesias-Bartolome et al., 2012). Additionally, a recent study demonstrates that autophagy, a cellular process inhibited by mTORC1, is required for satellite cell maintenance by preventing senescence (García-Prat et al., 2016). Because the *Pten* null satellite cells experience persistent activation of the Akt/mTORC1 pathway, one would predict that they should exhibit accelerated senescence during aging.

Interestingly, functions of Pten in satellite cells are similar to those of Spry1, an inhibitor of FGF signaling (Chakkalakal et al., 2012). Both *Spry1* KO and *Pten* KO in satellite cells result in the loss of quiescence, age-dependent depletion, and diminished regenerative capacity. Spry1 antagonizes FGF2 signaling, which is upregulated in the aged niche to disrupt muscle stem cell quiescence (Chakkalakal et al., 2012). Because Pten functions as an antagonist of insulin growth factor (IGF) signaling, these studies together highlight the role of inhibitors of growth factor signaling pathways in stem cell maintenance. Intrinsic molecular effectors, such as Spry1, Pten, and p38$\alpha\beta$/MAPK, may function as mediators of extrinsic signaling to control satellite cell homeostasis (Bernet et al., 2014; Brack and Muñoz-Cánoves, 2016; Chakkalakal et al., 2012; Shea et al., 2010).

As a tumor suppressor, mutation of PTEN in stem cells or its progenitors enforces proliferation and tumorigenesis (Hollander et al., 2011; Wang et al., 2006; Zhang et al., 2006). Rhabdomyosarcoma (RMS), a highly aggressive soft-tissue sarcoma in children, arises from abnormal growth of myogenic stem and progenitor cells (Blum et al., 2013; Rubin et al., 2011). A recent study uncovers a high frequency of PTEN mutations and methylation in embryonal RMS (Seki et al., 2015), thus pointing to a potential role of PTEN in regulating the growth and tumorigenic transformation of myogenic progenitors. However, RMS was never detected in our $Pten^{MKO}$ mice, not even in the aged mice. Although *Pten*-deficient myogenic progenitors exhibit accelerated proliferation, they subsequently differentiate and fuse into myofibers normally. Therefore, combined *Pten* loss of function and blockage of differentiation may be necessary for the pathogenesis of RMS.

Collectively, our study indicates that *Pten*-deficient myoblasts divide rapidly during perinatal growth, which results in muscle hypertrophy. On the other hand, *Pten* KO also accelerates age-dependent depletion of satellite cells. These observations point out a compensatory effect of intrinsic signaling on regulating stem cell homeostasis and tissue growth. That is, robust tissue growth at the expense of accelerated senescence of stem cells. Several factors, such as telomere length, mitochondrial activity, metabolic rates, and proliferative history, are known to influence stem cell aging (Beerman et al., 2013; Cerletti et al., 2012; Oh et al., 2014; Sahin and Depinho, 2010; Signer and Morrison, 2013). Therefore, it's interesting in the future to determine the exact cellular mechanism governed by Pten in regulating this compensatory effect of stem cell homeostasis and tissue growth.

EXPERIMENTAL PROCEDURES

Mice

All procedures involving mice were guided by the Purdue University Animal Care and Use Committee. All mouse strains were obtained from Jackson Laboratory under the following stock numbers: *MyoD*^{Cre} (#014140), *Pax7*^{CreER} (#012476), and *Pten*$^{f/f}$ (#006440). The genotypes of experimental knockout and associated control animals are as follows: *Pten*^{MKO} (*MyoD*^{Cre}::*Pten*$^{f/f}$), *Pten*$^{M+/-}$ (*MyoD*^{Cre}::*Pten*$^{+/f}$), and wild-type (*Pten*$^{f/f}$). For conditional *Pten* knockout in adult satellite cells, *Pax7*^{CreER}/*Pten*$^{f/f}$ and *Pten*$^{f/f}$ mice were injected intraperitoneally with 2 mg of tamoxifen (TMX) (Calbiochem) per day per 20 g of body weight for 5 days to induce Cre-mediated deletion. Mice were housed and maintained in the animal facility, with free access to standard rodent chow and water.

Muscle Injury and Regeneration

Muscle regeneration was induced by CTX injection. Adult mice were first anesthetized using a ketamine-xylazine cocktail, and CTX was injected (50 μL of 10 μM solution; Sigma) into the TA muscle. Muscles were then harvested at the indicated days post injection to assess the completion of regeneration and repair.

Treadmill Measurement

Mice were trained on a treadmill (Eco3/6 treadmill; Columbus Instruments) with a fixed 10% slope at a constant speed of 10 m/min for 5 min daily for 3 consecutive days before the test. On the exercise testing day, animals ran on the treadmill at 10 m/min for 5 min, and the speed was increased by 2 m/min every 2 min until they were exhausted or a maximal speed of 46 m/min was achieved. Exhaustion was defined as the inability of the animal to run on the treadmill for 10 s, despite mechanical prodding. Running time and maximum speed achieved were measured, whereas running distance was calculated.

Sciatic Nerve Denervation

For sciatic nerve denervation, mice were anesthetized with a ketamine-xylazine cocktail. The right hindlimb was prepared for surgery. Briefly, a 0.5-cm incision was made in the skin along the axis of the femur, and the sciatic nerve was isolated. To prevent reinnervation, a 3- to 5-mm section of sciatic nerve was cut and removed. Mice were sacrificed 3 weeks after denervation, and muscle samples were collected.

Primary Myoblast Isolation, Culture, and Differentiation

Satellite-cell-derived primary myoblasts were isolated from hindlimb skeletal muscles of *Pax7*^{CreER}/*Pten*$^{f/f}$ mice at the age of 6–8 weeks. Muscles were minced and digested in type I collagenase and Dispase B mixture (Roche). The digestions were stopped with F-10 Ham's medium containing 20% fetal bovine serum (FBS). Cells were then filtered from debris, centrifuged, and cultured in growth medium (F-10 Ham's medium supplemented with 20% FBS, 4 ng/mL basic FGF, and 1% penicillin-streptomycin) on collagen-coated cell culture plates at 37°C, 5% CO_2. For in vitro genetic deletion, *Pax7*^{CreER}/*Pten*$^{f/f}$ primary myoblasts were induced by 2 days of 4-OH tamoxifen (0.4 μM; Calbiochem), and the primary myoblasts treated with vehicle were set as the control.

For differentiation, primary myoblasts were seeded on BD Matrigel-coated cell culture plates and induced to differentiate in a low serum medium (DMEM supplemented with 2% horse serum and 1% penicillin-streptomycin). For reserve cell culture assay, low-passage primary myoblasts isolated from adult *Pax7*^{CreER}/*Pten*$^{f/f}$ mice were treated with control media or 4-OH-tamoxifen for 48 hr and then induced to differentiation at a low serum medium condition for 2.5 or 3.5 days with or without LY294002 (a potent PI3K inhibitor, 10 μM) or rapamycin (mTOR inhibitor, 25 nM).

Single Myofiber Isolation and Culture

Single myofibers were isolated from EDL muscles of adult mice (Pasut et al., 2013). Briefly, EDL muscles were dissected carefully and subjected to digestion with collagenase I (2 mg/mL, Sigma) in DMEM (Sigma) for 1 hr at 37°C. Digestion was stopped by carefully transferring EDL muscles to a pre-warmed Petri dish (60 mm) with 6 mL of DMEM, and single myofibers were released by gently flushing the muscles with a large bore glass pipette. The released single myofibers were then transferred and cultured in a horse-serum-coated Petri dish (60 mm) in DMEM supplemented with 20% FBS (HyClone), 4 ng/mL basic FGF (Promega), and 1% penicillin-streptomycin (HyClone) at 37°C.

Cell Cycle Entry Assay

Single myofibers isolated from WT and *Pten*^{MKO} mice were cultured in a horse-serum-coated Petri dish (60 mm) in DMEM supplemented with 20% FBS (HyClone), 4 ng/mL basic FGF (Promega), and 1% penicillin-streptomycin (HyClone) at 37°C. To monitor the cell cycle entry of satellite cells, EdU (Carbosynth) was added at a concentration of 1 μM into the culture medium. Cultured single myofibers were sampled at the indicated time.

Histology and Immunofluorescence Staining

Whole muscle tissues from WT and *Pten*^{MKO} mice were dissected and frozen immediately in an O.C.T. (optimum cutting temperature) compound. Frozen muscles were cross-sectioned (10 μm) using a Leica CM1850 cryostat. The slides were subjected to histological H&E staining or immunofluorescence staining. For immunofluorescence staining, cross-sections, single myofibers, or cultured cells were fixed in 4% paraformaldehyde (PFA) in PBS for 10 min, quenched with 100 mM glycine for 10 min, and incubated in blocking buffer (5% goat serum, 2% BSA, 0.1% Triton X-100, and 0.1% sodium azide in PBS) for at least 1 hr. Samples were then incubated with primary antibodies and then secondary antibodies and DAPI (see Supplemental Information for more details).

All images were captured using a Leica DM 6000B microscope, and images for WT and KO samples were captured using identical parameters. All the images shown are representative results of at least three biological replicates.

Statistical Analysis

The number of regenerated myofibers per mm^2 and the average CSA of regenerated fibers were calculated using Adobe Photoshop software. Muscle recovery rate was defined as the ratio of injured muscle to non-injured control muscle in the same mouse. All analyses were conducted with Student's t test, with a two-tail distribution. All experimental data are represented as mean ± SEM. Comparisons with p values < 0.05 were considered significant.

SUPPLEMENTAL INFORMATION

Supplemental Information includes Supplemental Experimental Procedures and seven figures and can be found with this article online at http://dx.doi.org/10.1016/j.celrep.2016.11.002.

AUTHOR CONTRIBUTIONS

F.Y. and S.K. conceived the project, designed the experiments, and prepared the manuscript. F.Y., P.B., C.W., and J.L. performed the experiments. J.L. and X.L. provided the reagents. F.Y. and S.K. analyzed the data.

ACKNOWLEDGMENTS

This work was supported by a grant from the US NIH (R01AR060652 to S.K.) and a Purdue incentive grant from the Purdue University Office of the Vice President for Research (OVPR) to S.K. We thank Dr. YongXu Wang (University of Massachusetts Medical School) for the generous present of the Adenovirus-AdEasy overexpression system, Dr. Shuichi Sato and Dr. Ashok Kumar (University of Louisville School of Medicine) for advice on treadmill experiments, Jun Wu for mouse colony maintenance, and members of the S.K. laboratory for valuable comments.

Received: May 17, 2016
Revised: September 19, 2016
Accepted: October 25, 2016
Published: November 22, 2016

REFERENCES

Almada, A.E., and Wagers, A.J. (2016). Molecular circuitry of stem cell fate in skeletal muscle regeneration, ageing and disease. Nat. Rev. Mol. Cell Biol. *17*, 267–279.

Beerman, I., Bock, C., Garrison, B.S., Smith, Z.D., Gu, H., Meissner, A., and Rossi, D.J. (2013). Proliferation-dependent alterations of the DNA methylation landscape underlie hematopoietic stem cell aging. Cell Stem Cell *12*, 413–425.

Bernet, J.D., Doles, J.D., Hall, J.K., Kelly Tanaka, K., Carter, T.A., and Olwin, B.B. (2014). p38 MAPK signaling underlies a cell-autonomous loss of stem cell self-renewal in skeletal muscle of aged mice. Nat. Med. *20*, 265–271.

Blau, H.M., Cosgrove, B.D., and Ho, A.T. (2015). The central role of muscle stem cells in regenerative failure with aging. Nat. Med. *21*, 854–862.

Blum, J.M., Añó, L., Li, Z., Van Mater, D., Bennett, B.D., Sachdeva, M., Lagutina, I., Zhang, M., Mito, J.K., Dodd, L.G., et al. (2013). Distinct and overlapping sarcoma subtypes initiated from muscle stem and progenitor cells. Cell Rep. *5*, 933–940.

Bodine, S.C., Stitt, T.N., Gonzalez, M., Kline, W.O., Stover, G.L., Bauerlein, R., Zlotchenko, E., Scrimgeour, A., Lawrence, J.C., Glass, D.J., et al. (2001). Akt/mTOR pathway is a crucial regulator of skeletal muscle hypertrophy and can prevent muscle atrophy in vivo. Nat. Cell Biol. *3*, 1014–1019.

Brack, A.S., and Muñoz-Cánoves, P. (2016). The ins and outs of muscle stem cell aging. Skelet. Muscle *6*, 1.

Brack, A.S., and Rando, T.A. (2012). Tissue-specific stem cells: lessons from the skeletal muscle satellite cell. Cell Stem Cell *10*, 504–514.

Cerletti, M., Jang, Y.C., Finley, L.W., Haigis, M.C., and Wagers, A.J. (2012). Short-term calorie restriction enhances skeletal muscle stem cell function. Cell Stem Cell *10*, 515–519.

Chakkalakal, J.V., Jones, K.M., Basson, M.A., and Brack, A.S. (2012). The aged niche disrupts muscle stem cell quiescence. Nature *490*, 355–360.

Chen, C., Liu, Y., Liu, R., Ikenoue, T., Guan, K.-L., Liu, Y., and Zheng, P. (2008). TSC-mTOR maintains quiescence and function of hematopoietic stem cells by repressing mitochondrial biogenesis and reactive oxygen species. J. Exp. Med. *205*, 2397–2408.

Cheung, T.H., and Rando, T.A. (2013). Molecular regulation of stem cell quiescence. Nat. Rev. Mol. Cell Biol. *14*, 329–340.

Collins, C.A., Zammit, P.S., Ruiz, A.P., Morgan, J.E., and Partridge, T.A. (2007). A population of myogenic stem cells that survives skeletal muscle aging. Stem Cells *25*, 885–894.

Dumont, N.A., Wang, Y.X., and Rudnicki, M.A. (2015). Intrinsic and extrinsic mechanisms regulating satellite cell function. Development *142*, 1572–1581.

García-Prat, L., Martínez-Vicente, M., Perdiguero, E., Ortet, L., Rodríguez-Ubreva, J., Rebollo, E., Ruiz-Bonilla, V., Gutarra, S., Ballestar, E., Serrano, A.L., et al. (2016). Autophagy maintains stemness by preventing senescence. Nature *529*, 37–42.

Gros, J., Manceau, M., Thomé, V., and Marcelle, C. (2005). A common somitic origin for embryonic muscle progenitors and satellite cells. Nature *435*, 954–958.

Hamilton, D.L., Philp, A., MacKenzie, M.G., and Baar, K. (2010). A limited role for PI(3,4,5)P3 regulation in controlling skeletal muscle mass in response to resistance exercise. PLoS ONE *5*, e11624.

Hollander, M.C., Blumenthal, G.M., and Dennis, P.A. (2011). PTEN loss in the continuum of common cancers, rare syndromes and mouse models. Nat. Rev. Cancer *11*, 289–301.

Iglesias-Bartolome, R., Patel, V., Cotrim, A., Leelahavanichkul, K., Molinolo, A.A., Mitchell, J.B., and Gutkind, J.S. (2012). mTOR inhibition prevents epithelial stem cell senescence and protects from radiation-induced mucositis. Cell Stem Cell *11*, 401–414.

Johnson, S.C., Rabinovitch, P.S., and Kaeberlein, M. (2013). mTOR is a key modulator of ageing and age-related disease. Nature *493*, 338–345.

Kanisicak, O., Mendez, J.J., Yamamoto, S., Yamamoto, M., and Goldhamer, D.J. (2009). Progenitors of skeletal muscle satellite cells express the muscle determination gene, MyoD. Dev. Biol. *332*, 131–141.

Kuang, S., and Rudnicki, M.A. (2008). The emerging biology of satellite cells and their therapeutic potential. Trends Mol. Med. *14*, 82–91.

Lai, K.-M.V., Gonzalez, M., Poueymirou, W.T., Kline, W.O., Na, E., Zlotchenko, E., Stitt, T.N., Economides, A.N., Yancopoulos, G.D., and Glass, D.J. (2004). Conditional activation of akt in adult skeletal muscle induces rapid hypertrophy. Mol. Cell. Biol. *24*, 9295–9304.

Lepper, C., Partridge, T.A., and Fan, C.-M. (2011). An absolute requirement for Pax7-positive satellite cells in acute injury-induced skeletal muscle regeneration. Development *138*, 3639–3646.

Liu, L., and Rando, T.A. (2011). Manifestations and mechanisms of stem cell aging. J. Cell Biol. *193*, 257–266.

Murphy, M.M., Lawson, J.A., Mathew, S.J., Hutcheson, D.A., and Kardon, G. (2011). Satellite cells, connective tissue fibroblasts and their interactions are crucial for muscle regeneration. Development *138*, 3625–3637.

Oh, J., Lee, Y.D., and Wagers, A.J. (2014). Stem cell aging: mechanisms, regulators and therapeutic opportunities. Nat. Med. *20*, 870–880.

Ortega-Molina, A., Efeyan, A., Lopez-Guadamillas, E., Muñoz-Martin, M., Gómez-López, G., Cañamero, M., Mulero, F., Pastor, J., Martinez, S., Romanos, E., et al. (2012). Pten positively regulates brown adipose function, energy expenditure, and longevity. Cell Metab. *15*, 382–394.

Pasut, A., Jones, A.E., and Rudnicki, M.A. (2013). Isolation and culture of individual myofibers and their satellite cells from adult skeletal muscle. J. Vis. Exp., e50074.

Relaix, F., Rocancourt, D., Mansouri, A., and Buckingham, M. (2005). A Pax3/Pax7-dependent population of skeletal muscle progenitor cells. Nature *435*, 948–953.

Rodgers, J.T., King, K.Y., Brett, J.O., Cromie, M.J., Charville, G.W., Maguire, K.K., Brunson, C., Mastey, N., Liu, L., Tsai, C.-R., et al. (2014). mTORC1 controls the adaptive transition of quiescent stem cells from G0 to G(Alert). Nature *510*, 393–396.

Rommel, C., Bodine, S.C., Clarke, B.A., Rossman, R., Nunez, L., Stitt, T.N., Yancopoulos, G.D., and Glass, D.J. (2001). Mediation of IGF-1-induced skeletal myotube hypertrophy by PI(3)K/Akt/mTOR and PI(3)K/Akt/GSK3 pathways. Nat. Cell Biol. *3*, 1009–1013.

Rubin, B.P., Nishijo, K., Chen, H.-I.H., Yi, X., Schuetze, D.P., Pal, R., Prajapati, S.I., Abraham, J., Arenkiel, B.R., Chen, Q.-R., et al. (2011). Evidence for an unanticipated relationship between undifferentiated pleomorphic sarcoma and embryonal rhabdomyosarcoma. Cancer Cell *19*, 177–191.

Sahin, E., and Depinho, R.A. (2010). Linking functional decline of telomeres, mitochondria and stem cells during ageing. Nature *464*, 520–528.

Sambasivan, R., Yao, R., Kissenpfennig, A., Van Wittenberghe, L., Paldi, A., Gayraud-Morel, B., Guenou, H., Malissen, B., Tajbakhsh, S., and Galy, A. (2011). Pax7-expressing satellite cells are indispensable for adult skeletal muscle regeneration. Development *138*, 3647–3656.

Sanchez-Gurmaches, J., Hung, C.-M., Sparks, C.A., Tang, Y., Li, H., and Guertin, D.A. (2012). PTEN loss in the Myf5 lineage redistributes body fat and reveals subsets of white adipocytes that arise from Myf5 precursors. Cell Metab. *16*, 348–362.

Seki, M., Nishimura, R., Yoshida, K., Shimamura, T., Shiraishi, Y., Sato, Y., Kato, M., Chiba, K., Tanaka, H., Hoshino, N., et al. (2015). Integrated genetic and epigenetic analysis defines novel molecular subgroups in rhabdomyosarcoma. Nat. Commun. *6*, 7557.

Serrano, A.L., Baeza-Raja, B., Perdiguero, E., Jardí, M., and Muñoz-Cánoves, P. (2008). Interleukin-6 is an essential regulator of satellite cell-mediated skeletal muscle hypertrophy. Cell Metab. *7*, 33–44.

Shea, K.L., Xiang, W., LaPorta, V.S., Licht, J.D., Keller, C., Basson, M.A., and Brack, A.S. (2010). Sprouty1 regulates reversible quiescence of a self-renewing adult muscle stem cell pool during regeneration. Cell Stem Cell *6*, 117–129.

Shefer, G., Van de Mark, D.P., Richardson, J.B., and Yablonka-Reuveni, Z. (2006). Satellite-cell pool size does matter: defining the myogenic potency of aging skeletal muscle. Dev. Biol. *294*, 50–66.

Signer, R.A., and Morrison, S.J. (2013). Mechanisms that regulate stem cell aging and life span. Cell Stem Cell *12*, 152–165.

Sousa-Victor, P., García-Prat, L., Serrano, A.L., Perdiguero, E., and Muñoz-Cánoves, P. (2015). Muscle stem cell aging: regulation and rejuvenation. Trends Endocrinol. Metab. *26*, 287–296.

Tajbakhsh, S. (2009). Skeletal muscle stem cells in developmental versus regenerative myogenesis. J. Intern. Med. *266*, 372–389.

Wang, S., Garcia, A.J., Wu, M., Lawson, D.A., Witte, O.N., and Wu, H. (2006). Pten deletion leads to the expansion of a prostatic stem/progenitor cell subpopulation and tumor initiation. Proc. Natl. Acad. Sci. USA *103*, 1480–1485.

White, R.B., Biérinx, A.-S., Gnocchi, V.F., and Zammit, P.S. (2010). Dynamics of muscle fibre growth during postnatal mouse development. BMC Dev. Biol. *10*, 21.

Wijesekara, N., Konrad, D., Eweida, M., Jefferies, C., Liadis, N., Giacca, A., Crackower, M., Suzuki, A., Mak, T.W., Kahn, C.R., et al. (2005). Muscle-specific Pten deletion protects against insulin resistance and diabetes. Mol. Cell. Biol. *25*, 1135–1145.

Yin, H., Price, F., and Rudnicki, M.A. (2013). Satellite cells and the muscle stem cell niche. Physiol. Rev. *93*, 23–67.

Zhang, J., Grindley, J.C., Yin, T., Jayasinghe, S., He, X.C., Ross, J.T., Haug, J.S., Rupp, D., Porter-Westpfahl, K.S., Wiedemann, L.M., et al. (2006). PTEN maintains haematopoietic stem cells and acts in lineage choice and leukaemia prevention. Nature *441*, 518–522.